

## Coupled plasmon and phonon excitations in the space-charge layer on GaAs(110) surfaces

Y. Chen, S. Nannarone,\* J. Schaefer,† J. C. Hermanson, and G. J. Lapeyre

*Department of Physics, Montana State University, Bozeman, Montana*

(Received 19 September 1988; revised manuscript received 18 November 1988)

High-resolution electron-energy-loss spectroscopy (HREELS) is used to study the surface plasmon and phonon in the space-charge layer on doped GaAs(110) cleaved surfaces. Three losses are observed, with energies of about 27, 36, and 42 meV. The peak at 36 meV is attributed to an un-screened phonon in the depletion layer. The other two losses are due to the coupled modes of the plasmon and phonon propagating near the interface of the depletion layer and the bulk. The surface Fermi-level pinning is induced either by residual-gas interaction with the surface or by deliberate hydrogen adsorption; this in turn modifies the depletion-layer thickness. This modification results in a quite pronounced change of the relative intensities and noticeable energy shifts of these losses. A model energy-loss spectrum calculated in the framework of local-response theory is used to deduce the properties of the space-charge layer. Our model is the first to use a self-consistent free-carrier profile together with the Lindhard description of the local dielectric response.

### INTRODUCTION

The study of III-V compound semiconductor surfaces has drawn much attention in the past decade due to their promising device-industry applications and interesting physical properties. Of particular interest from a physical standpoint is the surface plasmon, a collective excitation of the free carriers. The study of this excitation and its coupling with optical phonons and their interaction with a probing electron have been the subject of many experimental and theoretical investigations.<sup>1-14</sup>

In Ref. 2, Matz and Lüth first observed coupled phonon-plasmon modes on cleaved GaAs(110) surfaces by means of high-resolution electron-energy-loss spectroscopy (HREELS). But due to the doping level, the coupling was not very strong and the plasmon was very close to the elastic peak. Thus it was very difficult to carry out a systematic study during the depletion-layer formation process. In the present paper, we carry this study further by using the doping range where the coupling is the strongest. The interaction is more manifest and three peaks are observed due to this coupling. Thus the data provide an excellent reference for the testing of theoretical models. Also, we demonstrate more clearly the dramatic changes of the spectra due to residual-gas-surface interaction. These changes can be attributed to the surface Fermi-level pinning which causes the formation of a depletion layer. A self-consistent treatment of the depletion layer is used to interpret the data in terms of band-bending parameters.

### EXPERIMENTAL PROCEDURES AND RESULTS

The electron-energy-loss experiments on cleaved GaAs(110) surfaces were performed with a Leybold-Heraeus model ELS-22 spectrometer. The system also contains low-energy electron diffraction (LEED), electron spectroscopy for chemical analysis (ESCA), and ultraviolet photoelectron spectroscopy (UPS) facilities located in the

Center for Research in Surface Science (CRISS) at the Physics Department of Montana State University. The sample was supplied by Laser Diode, who measured the free-carrier mobility as  $1857 \text{ cm}^2/\text{V sec}$  and the bulk carrier density as  $1.3 \times 10^{18} \text{ cm}^{-3}$ . The crystals were cleaved by a single-wedge technique. The base pressure in the chamber was about  $5 \times 10^{-10}$  Torr during the experiment. The surface Fermi-level pinning was monitored by He uv-lamp photoemission spectroscopy. The hydrogen exposure was made by placing the surface at approximately 5 cm from a hot (2200 K) tungsten filament. The dose was recorded as molecular-gas exposure since the conversion rate is unknown. Because the spectrum is very sensitive with respect to time, as we will discuss later, both ion gauge and ion pump were turned off during the experiment to reduce the residual-gas-surface interaction.

A typical loss spectrum with 9 eV primary energy and  $45^\circ$  incident angle for these doped GaAs(110) surfaces after interacting with hydrogen is shown in Fig. 1. Three

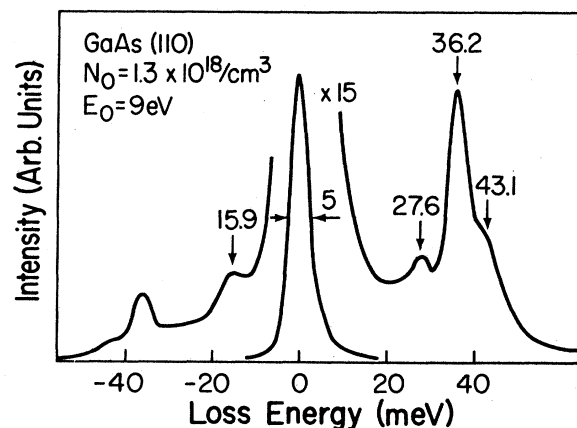


FIG. 1. Typical HREELS spectrum of *n*-type GaAs(110) after hydrogen exposure.

losses and corresponding gains at around 28, 36, and 43 meV are observed. In addition, a clearly resolved peak on the gain side with energy of about 16 meV is present. Due to higher background and an asymmetric elastic peak, this gain peak cannot be resolved on the loss side. When the sample was cooled down to 110 K this gain peak disappears while the other three losses remain the same. In Fig. 2, spectra at different stages are shown. On a fresh-cleaved surface (5 min after cleave) the loss energies of the three peaks are 27.7, 36.9, and 43.7 meV. The peak in the middle only appears as a shoulder. After the UPS spectrum was taken (35 min after cleave) the loss spectrum changed significantly. The middle peak grew higher, whereas the first peak shifted down about 1 meV and the third peak also shifted down 1 meV and reduced its intensity. Forty-five minutes after cleave, the spectrum changed again in the same way. At 500-L hydrogen exposure, the spectrum reached its final stage: The first peak was at 26.5 meV, the second peak became dominant at 36 meV, and the third peak was only a small shoulder. [1 langmuir (L)  $\equiv 20^{-6}$  Torr sec.] This spectrum is quantitatively different from the ir spectrum of similar measurements reported in Ref. 1, where the lower energy loss appeared at 33 meV and the higher energy loss at 44 meV is much more intense. The energy position and intensity of the coupled plasmon and phonon are very sensitive to

the space-charge parameters, as discussed later in the HREELS measurement. In the ir measurement, the probing depth is much larger; in addition, the loss function is the bulk type. Thus it is not surprising that the two probes do not provide quantitatively the same results.

Then the UPS spectrum was taken again and a total band bending of 0.42 eV was obtained. We attribute the dramatic changes of the loss spectrum as time elapses to residual-gas-surface interaction which alters the surface Fermi-level pinning. The same effect was observed in a separate experiment,<sup>8</sup> although the changes occurred much more slowly because the base pressure was about four times lower. At this stage, we cannot identify the species which interact with the surface although hydrogen is the most likely candidate. At any rate, our results demonstrate the sensitivity of HREELS data to space-charge-layer parameters.

After the hydrogen exposure, spectra with different primary energies were also taken, as shown in Fig. 3. The spectrum with 21 eV primary energy shows a somewhat reduced middle peak, whereas the spectrum with 4 eV primary energy has a much higher middle peak compared with the data in Fig. 1. These effects can be interpreted as the results of a larger probing depth for electrons with high impact energy.<sup>4,5,8</sup> The gain peak at 16 meV (not shown here) more or less follows the behavior of the 36-meV peak.

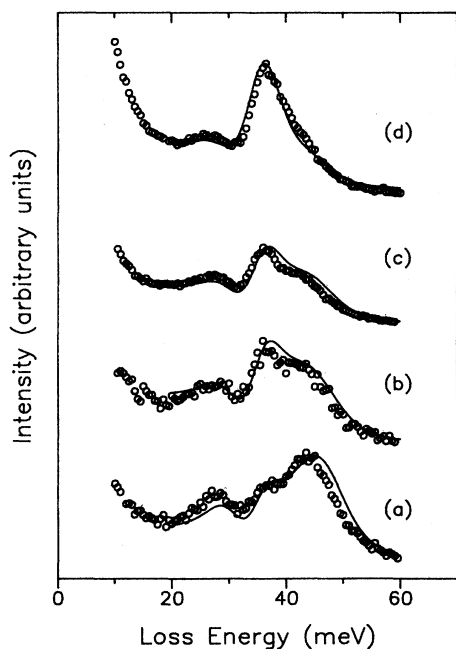


FIG. 2. The HREELS spectra of the cleaved GaAs(110) surface (open circle). The probing electron impinges on the surface with  $45^\circ$  incident angle and 9 eV primary angle. (a) 5 min after cleave, (b) 35 min after cleave, (c) 45 min after cleave, (d) after 500 L hydrogen exposure. The solid lines are the theoretical spectra.  $1.3 \times 10^{18} \text{ cm}^{-3}$  is the estimated bulk carrier concentration, and the depletion-layer thickness assumed for each spectrum is 70, 110, 125, and 230 Å, respectively.

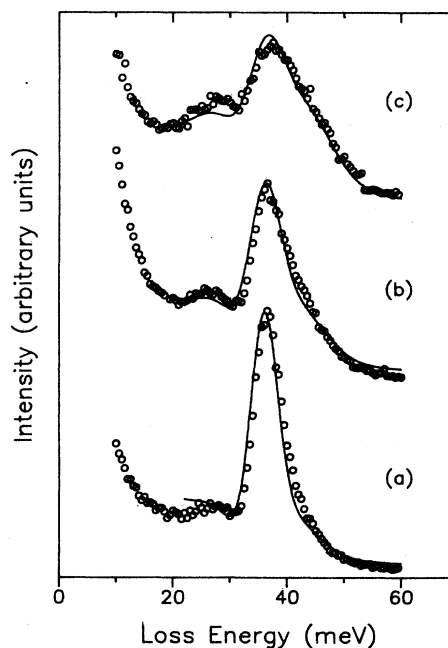


FIG. 3. The HREELS spectra for different primary energies after hydrogen exposure (open circle). The solid lines are calculated spectra with an estimated bulk carrier density of  $1.3 \times 10^{18} \text{ cm}^{-3}$  and a depletion-layer thickness of 230 Å. Primary energies are (a) 4 eV, (b) 9 eV, (c) 21 eV.

## ANALYSIS AND DISCUSSION

Free carriers in a doped semiconductor exhibit plasmon oscillations. This plasmon couples to the optical phonon, yielding two coupled modes or "plasmareons."<sup>2</sup> The loss spectrum is very sensitive to the free-carrier density and the details of the space-charge distribution.<sup>2,4,8</sup> In addition, a "dead layer," i.e., a layer near the surface where the carrier density is zero, has been suggested by a number of authors.<sup>3,4,8-14</sup> This important concept is based on a very fundamental quantum-mechanical effect. Conduction-band electrons in semiconductors are trapped in a potential well. The height of this well is several electron volts (the electron affinity), which is much higher than the electron kinetic energy, so that the electron wave function decays to zero within a few angstroms above the surface. Now the free carriers only occupy the very bottom of the conduction band in an  $n$ -type semiconductor. Thus the Fermi wavelength is much larger than the lattice constant. Vanishing wave function at the surface and long wavelength lead to an electron-free region near the surface, on the order of 50 Å at high doping levels, even in the absence of surface charge. The effect of the dead layer on HREELS is similar to that of a depletion layer caused by band bending. Note, however, that the dead layer, unlike a true depletion layer, has no net charge; the former should be described as a dipole layer. Nonetheless, the dead layer does produce a small band bending, even when the surface is neutral.

Intuitively, the depletion layer affects the spectrum in the following way. In the depletion layer, the optical phonon is unperturbed and oscillates without damping due to the absence of free carriers in this region. The thickness of this layer determines the total volume of the crystal which can be excited and therefore the intensity of the bare phonon. Below the depletion layer, the phonon couples strongly to the plasmon resulting in two new modes. These two modes not only depend on the electron concentration in the bulk but also on the environment; namely, the boundary condition. Different depletion-layer profiles define different plasmon-phonon modes. As a consequence, the loss features are sensitive, in energy position and intensity, to the space-charge distribution.

The most interesting feature in our spectra is the presence of the unscreened phonon at 36 meV even on the fresh-cleaved surface. To minimize the effect of the residual-gas-induced depletion layer, the first spectrum was taken within 5 min of the cleavage. Thus, the data provide definite evidence for the existence of an intrinsic electron-free region near the surface.

To study the space-charge layer in more detail, a theoretical calculation is useful. We have applied the dielectric theory<sup>15</sup> of HREELS as reformulated by Lambin *et al.*<sup>16</sup> to allow for continuous variation of the target's dielectric properties perpendicular to the surface. The latter authors derived an expression for the energy-loss spectrum in terms of an effective surface dielectric function  $\xi_0(k, \omega)$  determined by the solution of a Riccati differential equation. The major input to the Riccati equation is the local dielectric function  $\epsilon(k, \omega, z)$ , namely the bulk dielectric function evaluated at the local free-

carrier density  $n(z)$ , where  $z$  is the coordinate normal to the surface;  $k$  and  $\omega$  are the two-dimensional wave vector and the frequency. This model is valid at long wavelength (small  $k$ ), although nonlocal corrections<sup>14</sup> may be important for narrow depletion layers. For free-carrier densities of  $10^{18} \text{ cm}^{-3}$  or higher, the characteristic wave vector determined from the scattering kinematics is an order of magnitude smaller than the Fermi wave vector, so the long-wavelength model is appropriate.

The free-carrier profile  $n(z)$  was determined from self-consistent solutions of the Poisson and Schrödinger equations as outlined by Ehlers and Mills.<sup>13</sup> Fermi statistics at 300 K were used to describe the electrons in the conduction band. For bulk free-carrier densities  $n_0$  greater than  $10^{17} \text{ cm}^{-3}$  the donor binding energy vanishes due to screening effects, and a related insulator-metal transition occurs among the donor levels.<sup>17</sup> Thus we have assumed complete ionization of the donor levels at  $1.3 \times 10^{18} \text{ cm}^{-3}$ . To simplify solving the Schrödinger equation we modeled the doped semiconductor as a slab of thickness 100–1350 Å (the thickest depletion layer which we considered was 250 Å); we always obtained the bulk density  $n_0$  and Fermi level in the center of the slab. As in Ref. 13, surface charges were approximated as two-dimensional densities with no variation along the surface. We integrated the Schrödinger equation using a subroutine supplied by Numerical Algorithms Group (Downers Grove, IL) which solves the Sturm-Liouville problem using a Pruefer transformation and a shooting method. We then integrated the Riccati equation<sup>16</sup> for  $\xi(k, \omega)$ , which was inserted into the  $k$ -space integral for the loss spectrum. Because the plasmon-phonon coupled modes have energies near  $k_B T$ , the factor  $1 + n(\omega)$  was inserted into the loss function, where  $n(\omega)$  is the Bose-Einstein occupation number.

The energy-loss spectra we computed are sensitive to the dielectric response model used. In particular, the Drude model, which omits the wave-vector dependence of  $\epsilon(k, \omega)$ , gives a poor account of our data and disagrees with the full Lindhard response;<sup>18</sup> we return to this point later. On the other hand, the Thomas-Fermi dielectric model, which replaces the Lindhard dielectric function by its quadratic  $k$  dependence, yields spectra that agree reasonably well with the full theory, as does the Debye-Hückel model. The basic flaw in the Drude model in depletion layers is that its predicted surface-plasmon dispersion curve always bends downward due to the tendency for  $n(z)$  to decrease near the surface. The other dielectric models mentioned above include upward dispersion through the bulk response described by  $\epsilon(k, \omega)$ . The Lindhard model also includes a mechanism for electron-hole pair excitation, an effect which broadens and reduces the plasmon-loss intensity and adds a broad (though weak) continuum. Below we interpret the HREELS data on an  $n$ -type GaAs(110) surface using the complex Lindhard dielectric function  $\epsilon_{\text{RPA}}$ . Because  $\epsilon_{\text{RPA}}$  does not include electron-impurity scattering, we supplemented the imaginary part with a Drude-like term  $\omega_p^2 \alpha / \omega^3$ , where  $\omega_p$  is the unscreened plasma frequency and  $\alpha$  the electron-impurity scattering width determined from the mobility; in energy units  $\omega_p$  is 158 meV and  $\alpha$  is 9.1 meV. The in-

clusion of this new term is essential since it broadens the plasmon-loss features significantly. Note that we have assumed that pair excitation and electron-impurity scattering are independent in this formulation.

The input parameters for the model calculations are the bulk free-carrier density  $1.3 \times 10^{18} \text{ cm}^{-3}$  measured by the crystal grower, the effective mass 0.0715 at the Fermi energy,<sup>19</sup> the dielectric constants 10.9 and 12.9 for low and high frequencies compared with the optical-phonon frequency  $\omega_{LO}$ , and the lattice contribution to dielectric response

$$\epsilon_L(\omega) = 10.9 - \frac{2.0\omega_{TO}^2}{\omega^2 - \omega_{TO}^2 + i\omega g}, \quad (1)$$

where  $\omega_{TO} = 36.1 \text{ meV}$  and  $g = 0.3 \text{ meV}$ , as inferred from infrared data. We used the static dielectric function 12.9 in the self-consistent charge-density calculations; it enters the Poisson equation on the right-hand side.<sup>13</sup> The input dielectric function for the Ricatti equation is

$$\epsilon(k, \omega, z) = \epsilon_L(\omega) + [\epsilon_{RPA}(k, \omega, z) - 1] + i\omega_p^2 \alpha / \omega^3. \quad (2)$$

Since the angular acceptance at the detector is  $1^\circ$ – $2^\circ$ , essentially all dipole-allowed<sup>15</sup> scattering events are counted when the detector axis coincides with the specular direction; thus we extended the integral for the loss spectrum to large values of  $k$  on the order of 10.

Our depletion layer models are labeled by the effective depletion depth

$$D = Q / n_0, \quad (3)$$

where  $Q$  is the surface charge density, defined as a positive quantity. To obtain  $Q$  from the quoted values of  $D$  (in units of angstrom), use the formula

$$Q = 1.3 \times 10^{10} D (\text{\AA}) \text{ cm}^{-2}. \quad (4)$$

The energy-loss spectra for a series of depletion-layer thicknesses are compared with HREELS data in Figs. 2 and 3. In fitting the theoretical model to the data we allowed for an overall scale adjustment and a weak constant background in each curve. We studied a range of depletion-layer depths from 0 to 250  $\text{\AA}$  but did not attempt to adjust the bulk density  $n_0$  or the mobility specified by the supplier. In retrospect, a slightly smaller value of  $n_0$  might improve our fits. Figure 2 presents results for an electron kinetic energy of 9 eV and an angle of incidence of  $45^\circ$ ; the changing experimental parameter is exposure. Figures 3(a)–3(c) were all obtained at saturation coverage of atomic hydrogen but for kinetic energies of 4, 9, and 21 eV. Note that Figs. 2(d) and 3(b) are identical. The theoretical curves were broadened by Gaussian convolution using a FWHM of 5–7 meV estimated from the quasielastic peak, whose asymmetry we ignored.

Even on a fresh-cleaved GaAs(110) surface, where the flat-band condition is expected, a finite depletion layer (70  $\text{\AA}$ ) is needed to fit the data; see Fig. 2(a). This discrepancy could arise from the fact that a bad cleave can induce initial band bending which causes depletion-layer forma-

tion. However, this cause seems unlikely because we have found no cleavage that yielded a thinner depletion layer. Note that a 70- $\text{\AA}$  depletion layer only requires a band bending of 0.07 eV, which is near the instrumental limit. On the other hand,  $9.1 \times 10^{11} \text{ cm}^{-3}$  surface charge deduced from 70  $\text{\AA}$ , which is about 0.001 electrons per surface atom, seems too large. The overestimate of the initial depletion layer might be due to the local dielectric description, since the charge density is very nonuniform near the surface when there is no surface charge. As residual-gas exposure increases in Figs. 2(a)–2(c),  $D$  grows in a nearly linear fashion, increasing from 70 to 100  $\text{\AA}$  in 30 min and then from 100 to 125  $\text{\AA}$  in 10 min. Thus the surface charge increases at a nearly constant rate at low exposure. At saturation coverage [Fig. 2(d)] a good fit is obtained for  $D = 230 \text{ \AA}$ ; the corresponding band bending is 0.52 eV, which is close to that inferred from the Fermi-level pinning value reported by Bartels *et al.*<sup>20</sup>, 0.55 eV, for saturated hydrogen chemisorption on cleaved *n*-type GaAs(110). We obtained an independent estimate of this quantity from UPS measurements of the Ga 3*d* core line. Due to the relatively rapid change of the band bending, only two UPS spectra were taken: one 25 min after the cleave and one after 500-L  $\text{H}_2$  exposure when the band bending has saturated. A total band-bending shift of 0.42 eV occurs between these spectra. The model calculations predict the value 0.38 eV for this shift.

As noted above, the model spectra depend on the specific dielectric function used in the Ricatti equation. Figure 4 demonstrates this by comparing the results we obtained for the energy-loss spectrum using four different dielectric models. The parameters were chosen to correspond to Fig. 2(b), and indeed the solid curve in Fig. 4 is the Lindhard result displayed in the earlier figure. The

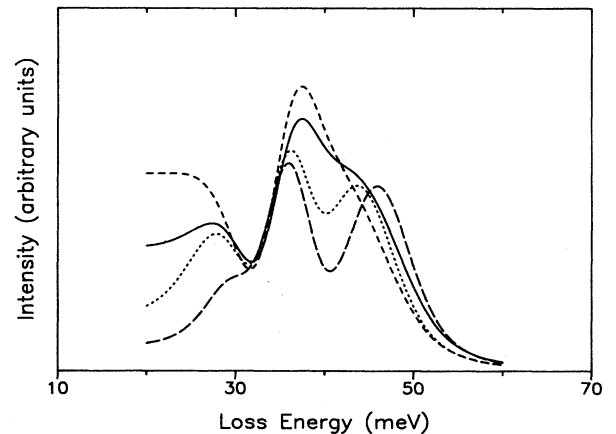


FIG. 4. The calculated HREELS spectra for various models of the free-carrier profile and dielectric response. The solid curve is the same as in Fig. 2(b), with a depletion-layer depth of 110  $\text{\AA}$  and an incident-electron kinetic energy of 9 eV. When the full Lindhard response is replaced by the Drude model, the dashed curve is predicted. The remaining two spectra are obtained when the self-consistent free-carrier profile is replaced with a step function; the long-dashed (dotted) curve is predicted by the Lindhard (Drude) dielectric model.

spectrum obtained from the self-consistent charge density but using the Drude model of dielectric response has a much weaker shoulder on the high-energy side of the unscreened-phonon peak, while the low-energy peak is too strong. In the Drude model,  $\epsilon_{\text{RPA}}(k, \omega, z)$  is replaced by

$$\epsilon_D(\omega, z) = 1 - \omega_p^2(z) / (\omega^2 + i\omega\alpha). \quad (5)$$

The remaining two curves in Fig. 4 were computed using the widely employed<sup>3-8</sup> Schottky depletion-layer model, which approximates the free-carrier profile as a step function; i.e., the bulk density is assumed below the depth  $D$ , above which the density vanishes. In the step model both Lindhard and Drude dielectric functions lead to spectra that are too narrow; surprisingly, Drude response predicts peak positions in better agreement with the full theory. None of the approximate models give a satisfactory fit to our data. The failure of Drude response is due to the negative dispersion relation it predicts. The step profile fails because it contains no regions of intermediate charge density that would broaden the plasmon energy on the low-energy side; it leads to narrow peaks at higher energy. Combining Drude response and the step profile produces a partial compensation of errors. The deficiencies of these models were manifest in our analysis because of the delicate interplay of nearly degenerate excitations. In general, the predictions of the approximate models should be treated with caution.

Finally, we would like to comment on the 16-meV gain peak observed. This peak is not an artifact of spectrometer tuning, since it is observed on two spectrometers and by another lab.<sup>21</sup> It is also unlikely that this peak is anomalous, in the sense that only its gain is observed. In fact, the elastic peak is asymmetric and the background on the loss side is higher; therefore the loss peak of this resonance is probably buried in the background. In addition, this gain peak disappeared when the sample was cooled down to 80 K, providing evidence that this is a normal dipole excitation. The intensity of this peak is so strong it only can be a collective excitation. The fact that its intensity does not change like that of a plasmon with respect to primary energy could mean that the excitation

has a different spatial structure. Moreover, since surface contamination does not change this peak, the excitation is probably not the type of surface phonon found on Si(111).<sup>22</sup> Based on this analysis, we suggest that this peak is due to a surface optical mode. Recently, Harten *et al.* reported an observation of two flat optical modes at 10 and 13 meV in their helium-atom-scattering experiments on GaAs(110).<sup>23</sup> These two modes are yet to be understood, although they can be interpreted in terms of localized atomic vibrations. The mode observed in our experiments is at slightly higher energy and the dispersion was not measured, thus we cannot conclude that this is the same mode they observed. Both results suggest that surface phonon structures exist besides the Fuchs-Kleiwier phonon. More measurement and theoretical calculations need to be done to address this issue.

### SUMMARY

A HREELS study of the plasmon and phonon modes in the space-charge layer of the GaAs(110) surface was performed. Three losses were observed which can be attributed to the coupled modes of plasmons and phonons on the "interface" of depletion layer and bulk and to the unscreened phonon mode in the depletion layer. A self-consistent free-carrier profile was obtained for various surface charge densities and energy-loss spectra were calculated in the framework of semiclassical local-response theory. Good line-shape fits were obtained for all spectra. The model parameters contain information about the space-charge profile and band bending. The band bending inferred after 500 L H<sub>2</sub> exposure is in good agreement with our UPS measurement and with an earlier result.<sup>20</sup>

### ACKNOWLEDGMENTS

We express our appreciation for the support of J. R. Anderson and Milt Jaehnig and many helpful discussions with Professor A. G. Eguluz. This research is supported by the National Science Foundation under Grant No. DMR-83-09460.

\*Permanent address: Prima Università degli Studi di Roma, La Sapienza, I-00185 Roma, Italy.

†Permanent address: Gesamthochschule Kassel, Postfach 101380 D-3500, Kassel, West Germany.

<sup>1</sup>A. Pinczuk, G. Abstreiter, R. Trommer, and M. Cardona, *Solid State Commun.* **21**, 959 (1977).

<sup>2</sup>R. Matz and H. Lüth, *Phys. Rev. Lett.* **46**, 500 (1981).

<sup>3</sup>I. Egri, R. Matz, H. Lüth, and A. Stahl, *Surf. Sci.* **128**, 51 (1983).

<sup>4</sup>A. Ritz and H. Lüth, *Phys. Rev. Lett.* **52**, 1242 (1984).

<sup>5</sup>Z. J. Gray-Grychowski, R. G. Egdell, B. A. Joyce, R. A. Stradling, and K. Woodbridge, *Surf. Sci.* **186**, 482 (1987).

<sup>6</sup>Joseph A. Stroschio and W. Ho, *Phys. Rev. Lett.* **54**, 1573 (1985).

<sup>7</sup>L. H. Dubois, B. R. Zegarski, and B. N. J. Persson, *Phys. Rev.*

**B 35**, 9128 (1987).

<sup>8</sup>Yu Chen, Yabo Xu, and G. J. Lapeyre, *J. Vac. Sci. Technol. A* **6**, 686 (1988).

<sup>9</sup>Joel I. Gersten, *Surf. Sci.* **97**, 206 (1980).

<sup>10</sup>A. Stahl, *Surf. Sci.* **134**, 297 (1983).

<sup>11</sup>W. L. Schaich, *Surf. Sci.* **134**, 297 (1983).

<sup>12</sup>W. L. Schaich, *Phys. Rev. Lett.* **53**, 2059 (1984).

<sup>13</sup>D. H. Ehlert and D. L. Mills, *Phys. Rev. B* **34**, 3939 (1986).

<sup>14</sup>D. H. Ehlert and D. L. Mills, *Phys. Rev. B* **36**, 1051 (1987).

<sup>15</sup>A. A. Lucas and M. Sunjii, *Prog. Surf. Sci.* **2**, 75 (1972); *Surf. Sci.* **32**, 439 (1972).

<sup>16</sup>Ph. Lambin, J. P. Vigneron, and A. A. Lucas, *Phys. Rev. B* **32**, 8203 (1985).

<sup>17</sup>P. P. Edwards and M. J. Sienko, *Phys. Rev. B* **17**, 2575 (1978).

<sup>18</sup>A. L. Fetter and J. D. Walecka, *Quantum Theory of Many-*

- Particle Systems* (McGraw-Hill, New York, 1971).
- <sup>19</sup>A. Raymond, J. L. Robert, and C. Bernard, *J. Phys. C* **12**, 2289 (1979).
- <sup>20</sup>F. Bartels, L. Surkamp, H. J. Clemens, and W. Mönch, *J. Vac. Sci. Technol. B* **1**, 756 (1983).
- <sup>21</sup>Maria Grazia Betti (private communication).
- <sup>22</sup>H. Ibach, *Phys. Rev. Lett.* **27**, 253 (1971).
- <sup>23</sup>V. Harten and J. P. Toennies, *Europhys. Lett.* **4**, 833 (1987).